

# Magnetic proximity effect in Perovskite Superconductor/Ferromagnet Multilayers

J. Stahn<sup>1</sup>, J. Chakhalian<sup>2</sup>, Ch. Niedermayer<sup>1</sup>, J. Hoppler<sup>1</sup>, T. Gutberlet<sup>1</sup>, J. Voigt<sup>1</sup>,

F. Treubel<sup>3</sup>, H-U. Habermeier<sup>2</sup>, G. Cristiani<sup>2</sup>, B. Keimer<sup>2</sup> and C. Bernhard<sup>2</sup>

<sup>1</sup>*Laboratorium für Neutronenstreuung, ETH Zürich & PSI, Villigen, Switzerland*

<sup>2</sup>*Max Planck Institut für Festkörperforschung, Stuttgart, Germany and*

<sup>3</sup>*Fakultät für Physik, Universität Konstanz, Germany*

(Dated: July 24, 2021)

YBa<sub>2</sub>Cu<sub>3</sub>O<sub>7</sub>/La<sub>2/3</sub>Ca<sub>1/3</sub>MnO<sub>3</sub> superconducting/ferromagnetic (SC/FM) multilayers have been studied by neutron reflectometry. Evidence for a characteristic difference between the structural and magnetic depth profiles is obtained from the occurrence of a structurally forbidden Bragg peak in the FM state. The comparison with simulated reflectivity curves allows us to identify two possible magnetization profiles: a sizable magnetic moment within the SC layer antiparallel to the one in the FM layer (inverse proximity effect), or a “dead” region in the FM layer with zero net magnetic moment. The former scenario is supported by an anomalous SC-induced enhancement of the off-specular reflection, which testifies to a strong mutual interaction of SC and FM order parameters.

PACS numbers: 74.81.-g, 74.78.Fx, 74.48.+c, 73.21.Ac, 61.12.Ha

Recent advances in fabrication and characterization of multilayers with nanoscale periodicity based on perovskite oxides have opened a new avenue in the investigation of materials with strong electron correlations [1]. Superlattices composed of ferromagnets (FM) and superconductors (SC) are of particular interest because their mutually exclusive ground state properties can give rise to novel quantum phenomena [2]. Prominent examples are the so-called  $\pi$ -junction effect [3], where the phase of the SC order parameter is modulated across the layers, or states with a spatial modulation of the amplitudes of the FM and SC order parameters such as spontaneous vortex phases or the Larkin-Ovchinnikov-Fulde-Ferrel (LOFF) state. Experimental signatures include a non-trivial dependence of  $T_c$  on the FM layer thickness [4, 5] and a complex magnetic phase diagram with reentrant SC states.

Extensive earlier work on classical metallic FM/SC multilayers has verified the  $\pi$ -junction effect, whereas a LOFF pairing state has not yet been firmly established. The work on the perovskite oxide FM/SC superlattices is motivated by the appealing properties of the cuprate high  $T_c$  superconductors (HTSC) whose high SC critical temperatures make them potentially useful for technological applications. Further, since HTSC are believed to be susceptible to a variety of competing instabilities, there is a high potential for novel SC/FM quantum states in multilayer structures. This research is in its early stage, and relatively little is known about the nature of magnetism at the interface, the spatial distribution of the magnetization throughout the layers, and the interplay of FM and SC order parameters in general. Neutron reflectivity has been a tool of choice in investigating interfaces in thin films and multilayers [6, 7]. In general, it allows one to probe a potential normal to the surface which consists of the contributions from the atomic nuclei  $V_{\text{nuc}}(z)$  and the magnetic potential  $V_{\text{mag}}(z)$ . A periodic

multilayer can be regarded as a one-dimensional crystal which gives rise to Bragg peaks that provide information on the number of layers from the peak width, the period length from the distance between adjacent peaks, and the ratio of the individual layer thicknesses from the relative peak intensities. In addition, the in-plane (“off-specular”) width of the peaks yields information about the in-plane magnetization profile. This technique has provided valuable information on the microscopic magnetic properties of classical FM/SC multilayers, but has so far not been successfully applied to perovskite oxide FM/SC multilayers.

In this letter we report the first results of polarized and unpolarized neutron reflectivity measurements on symmetric superlattices (with identical LCMO and YBCO layer thicknesses) that consist of alternating layers of the FM colossal magneto-resistance material La<sub>2/3</sub>Ca<sub>1/3</sub>MnO<sub>3</sub> (LCMO) and the HTSC compound YBa<sub>2</sub>Cu<sub>3</sub>O<sub>7</sub> (YBCO). Symmetric superlattices are well suited to explore a possible interference between SC and FM order parameters, because an extinction rule disallows all even-order Bragg reflections if  $V_{\text{mag}}(z)$  is spatially uniform and confined to the LCMO layer. The reflectivity curves above the FM and SC transitions ( $T > T_{\text{mag}}$  and  $T_{\text{sc}}$ ) indeed exhibit only odd-numbered Bragg peaks and testify to the high structural quality of our superlattices (with an rms interface roughness [7] of  $\sigma \approx 5 \text{ \AA}$ ). The reflectivity curves exhibit marked changes in the FM state as well as in the SC state. In particular, the appearance of a second-order magnetic Bragg peak below  $T_{\text{mag}}$  indicates that  $V_{\text{mag}}(z)$  either reaches into the YBCO layer with antiferromagnetic coupling across the interface or is confined to a spatial range significantly less than the thickness of the LCMO layer. Both scenarios are incompatible with a conventional magnetic proximity effect as proposed in Refs. [8, 9]. An anomalous enhancement of the off-specular reflection in the SC state

indicates a strong mutual interaction of SC and FM order parameters. This lends support to the former model, where the SC and FM order parameters are in intimate contact, and disfavors the latter one, where they are separated by a magnetically “dead” region.

Superlattices of [LCMO(98 Å)/YBCO(98 Å)]<sub>7</sub> (sample 1) and [LCMO(160 Å)/YBCO(160 Å)]<sub>6</sub> (sample 2) were grown by pulsed laser deposition (PLD) on  $10 \times 10 \times 0.5 \text{ mm}^3$  SrTiO<sub>3</sub> (001) substrates [5]. Their high quality was confirmed by x-ray diffraction, which showed epitaxial growth of the films with the  $c$ -axis along (110). Resistivity and SQUID magnetization measurements revealed a FM transition at  $T_{\text{mag}} \approx 165 \text{ K}$  and the onset of SC at  $T_{\text{sc}} \approx 75 \text{ K}$ . These values are substantially reduced from the typical bulk values of  $T_{\text{mag}}^{\text{LCMO}} = 270 \text{ K}$  and  $T_{\text{sc}}^{\text{YBCO}} = 93 \text{ K}$ , likely due to the proximity effect. [4, 5]

Unpolarized and polarized angle-dispersive neutron reflectivity measurements have been performed on the 2-axes diffractometers Morpheus at SINQ and ADAM at ILL. The polarized neutrons were reflected from the superlattice into a <sup>3</sup>He detector. The samples were mounted in a closed-cycle refrigerator with a temperature range from 12 to 300 K. The external magnetic field  $H_{\text{ext}}$  produced by Helmholtz coils was oriented perpendicular to the scattering plane and parallel to the film surface.

Figure 1(a) displays unpolarized neutron reflectivity curves taken under specular condition. The intensity of the 1st Bragg peak (averaged over the neutron spin states) exhibits a sizable increase below  $T_{\text{mag}}$ . This shows that the magnetic potential  $V_{\text{mag}}(z)$  enhances the contrast between the YBCO and LCMO layers, as expected due to the onset of magnetic order in LCMO. However, the 1 : 1 ratio of the layer thicknesses dictates that the even-order Bragg peaks should not be observable if the FM order parameter is either absent, or spatially uniform and confined to the LCMO layer. This condition is fulfilled for the curves at  $T > T_{\text{mag}}$  where the 2nd Bragg peak at  $q_z \sim 0.07 \text{ \AA}^{-1}$  (as marked by the shaded area) is absent to within the noise level. Below  $T_{\text{mag}}$ , however, the 2nd Bragg peak suddenly appears. The magnetic origin of the 2nd Bragg peak (confirmed by the polarized-beam data below) is indicative of a substantial difference between the spatial profiles of the nuclear and magnetic potentials.

A second kind of remarkable anomaly occurs in the vicinity of the SC transition. It is best seen in the off-specular rocking scans at the Bragg positions, as shown in Figures 1(b) and (c). The off-specular reflectivity is sensitive to a momentum transfer parallel to the plane of the multilayer ( $q_x$ ) and thus provides information on *in-plane* correlation of the nuclear and magnetic profiles. The left panel of Fig. 1(b) shows that the off-specular scattering is weak and nearly temperature independent

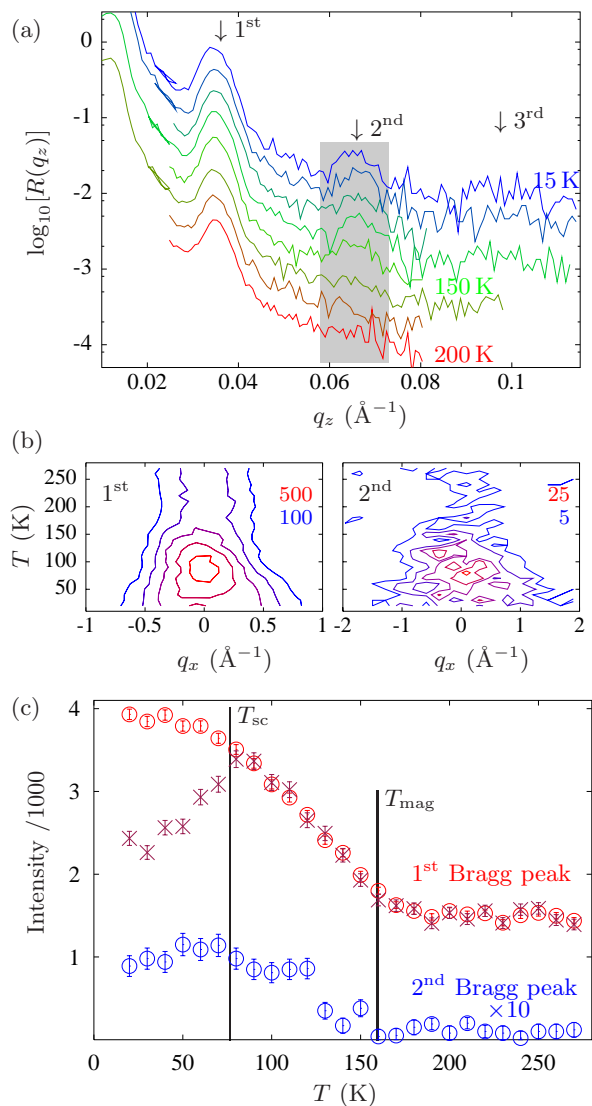


FIG. 1: (a) Specular reflectivity of sample 1 at 200, 170, 150, 120, 100, 70, 50 and 15 K, for  $H_{\text{ext}} = 100 \text{ Oe}$  (field cooled). Curves are offset for clarity. Bragg peaks are marked by arrows. (b)  $I(q_x, T)$  map for the 1st (left) and 2nd (right) Bragg peaks. (c)  $T$  dependence of the 1st (red) and 2nd (blue) Bragg peak intensities, integrated over  $q_x$  ( $\circ$ ) and at  $q_x = 0$  ( $\times$ , scaled by 6).

for  $T > T_{\text{mag}}$ . Such diffuse scattering is characteristic of uncorrelated in-plane roughness of the nuclear potential.

Below  $T_{\text{sc}}$ , however, a pronounced broadening occurs, and weight is transferred from the specular to the off-specular part. This is readily visible in Fig. 1(c) where the specular intensity (*crosses*) of the 1st Bragg exhibits a strong decrease, whereas the intensity integrated along  $q_x$  (*circles*) increases. The observed trend is indicative of a profound SC-induced increase in the magnetic roughness. A corresponding trend is observed for the 2nd Bragg peak as shown in the right panel of Fig. 1(b). For the 1st Bragg peak we estimate a change of the

full-width at half maximum  $\Delta q_x$  from  $0.6 \cdot 10^{-4} \text{ \AA}^{-1}$  (close to the instrumental resolution) at 75 K to about  $1.2 \cdot 10^{-4} \text{ \AA}^{-1}$  at 15 K. This translates into a change of the characteristic magnetic domain size from more than  $15 \mu\text{m}$  at  $T \simeq T_{\text{sc}}$  to about  $7 \mu\text{m}$  at  $T \ll T_{\text{sc}}$ . These pronounced SC-induced changes of the in-plane component of the magnetic profile are suggestive of a sizable proximity coupling of the SC and FM order parameters. SQUID magnetization data (not shown) indicate that the FM magnetic moments are oriented parallel to the layers of our superlattices. Orbital effects of the magnetic field in the SC layers are therefore expected to be weak, and the dominant interaction is the magnetic exchange coupling. This introduces a spin-splitting of the electronic states and reduces the SC condensation energy. In return, the development of the SC order parameter favors the formation of FM domain boundaries where the pair-breaking is substantially reduced [10]. The anomalous decrease in the size of the FM domains therefore provides a clear indication for a strong proximity coupling between the SC and FM order parameters. A spontaneous vortex phase (due to a minor perpendicular component of the FM moments) in the SC layers or the presence of an unconventional SC order parameter with a spin-triplet component could also contribute to the off-specular signal [11]. These scenarios could be tested by mapping out the off-specular signal in further experiments with an improved signal-to-noise ratio.

We now describe a quantitative analysis of the magnetization profile perpendicular to the layers. We tested numerous models with the EDXR code [7] that allows one to compare the calculated reflectivity curves with the experimental ones. In order to separate structural and magnetic contributions and to determine the quality of the interface, the nuclear contribution  $V_{\text{nuc}}(z)$  was determined from the curves at  $T > T_{\text{mag}}$ . The obtained individual layer thicknesses are  $98 \text{ \AA}$  and  $160 \text{ \AA}$  respectively, for samples 1 and 2. The density for LCMO was reduced by 2% with respect to the bulk value. The interface was described by a roughness of  $\sigma \approx 5 \text{ \AA}$ , which testifies to the high quality of our superlattices. It is well known that neutron reflectivity curves lack phase information and thus cannot be uniquely assigned to a particular density or magnetization profile. Nevertheless, we are able to identify only two possible solutions. The main challenge in selecting an appropriate magnetization profile is to reproduce the well-defined 1st structural Bragg peak, the magnetically induced 2nd Bragg peak, and the low intensity of the 3d structural Bragg peak. An extra constraint is imposed by the marked differences in polarized up-spin and down-spin reflectivities as shown in Fig. 2(a). While a wide variety of models are able to reproduce the 1st Bragg peak, the presence of the 2nd peak demonstrates that the magnetic potential  $V_{\text{mag}}(z)$  cannot simply follow the block-like nuclear profile. In the calculations,

the homogeneous magnetization of YBCO and LCMO layers was replaced by 48 slices of equal thickness with individually varying magnetization. Based on extensive computer simulations, we were able to exclude several physically meaningful models: (i) An antiferromagnetic coupling between the ferromagnetic layers would lead to a doubled period and hence to additional Bragg peaks, at  $q_z = 0.022 \text{ \AA}^{-1}$  and at  $q_z = 0.053 \text{ \AA}^{-1}$  which are absent in the reflectivity curves. (ii) A magnetic roughness of any length-scale only leads to a faster decay of the reflectivity but not to a second Bragg peak. (iii) A conventional magnetic proximity effect where the magnetization exhibits an exponential decay into the SC layer also fails.

In the following we discuss the only two successful models for which the magnetization profiles are illustrated in Fig. 2(c). Model 1 (*left panel*) contains a sizable magnetic moment within the YBCO layer that couples antiferromagnetically to the one in LCMO (inverse proximity effect). Notably, the antiparallel alignment is essential to reproduce the observed 2nd Bragg peak positions and intensities. Model 2 (*right panel*) assumes a “dead” region with no net magnetic moment (either paramagnetic or antiferromagnetic) within the LCMO layer. The resulting fits of the polarized reflectivities using model 1 are shown in Fig. 2(b). The values of the magnetic induction thus obtained are  $B_{\text{YBCO}} = 0.6 \text{ T}$  and  $B_{\text{LCMO}} = 0.9 \text{ T}$  (sample 1) and  $B_{\text{YBCO}} = 0.6 \text{ T}$  and  $B_{\text{LCMO}} = 1.4 \text{ T}$  (sample 2). The penetration depth of the interfacial magnetization profile is of the order of  $20 \text{ \AA}$  in the YBCO layer, and  $10 \text{ \AA}$  in the LCMO layer. Similar fits were obtained with model 2 (not shown) assuming a thickness of the “dead layer” of  $\approx 20 \text{ \AA}$  and magnetic induction  $B$  of  $1.1 \text{ T}$  (sample 1) and  $1.5 \text{ T}$  (sample 2).

While the model calculations do not allow one to differentiate between these two cases, we argue that the anomalous  $T$ -dependence in the SC state is a clear indication for a strong mutual interaction between the SC and FM order parameters and thus strongly favors model 1, which implies close contact between the SC and FM order parameters. First, we point out that the combined results of x-ray diffraction, electron microscopy [5] and in particular neutron reflectivity curves for  $T > T_{\text{mag}}$  testify to the high quality of the interfaces with practically absent inter-growth and small overall structural roughness of the order of  $5 \text{ \AA}$ . The magnetic profiles deduced from our neutron reflectivity data are therefore not merely due to interfacial disorder like inter-growth or inter-diffusion. One might argue that the magnetically “dead layer” in LCMO, the centerpiece of model 2, could arise from interfacial strain or charge transfer across the interface. According to the phase diagram of LCMO, this could introduce an insulating layer with antiferromagnetic order. However, such a “dead layer” would also efficiently reduce the exchange coupling between the SC and FM order parameters. Since the FM moments are oriented parallel to the layers (as demonstrated by SQUID mag-

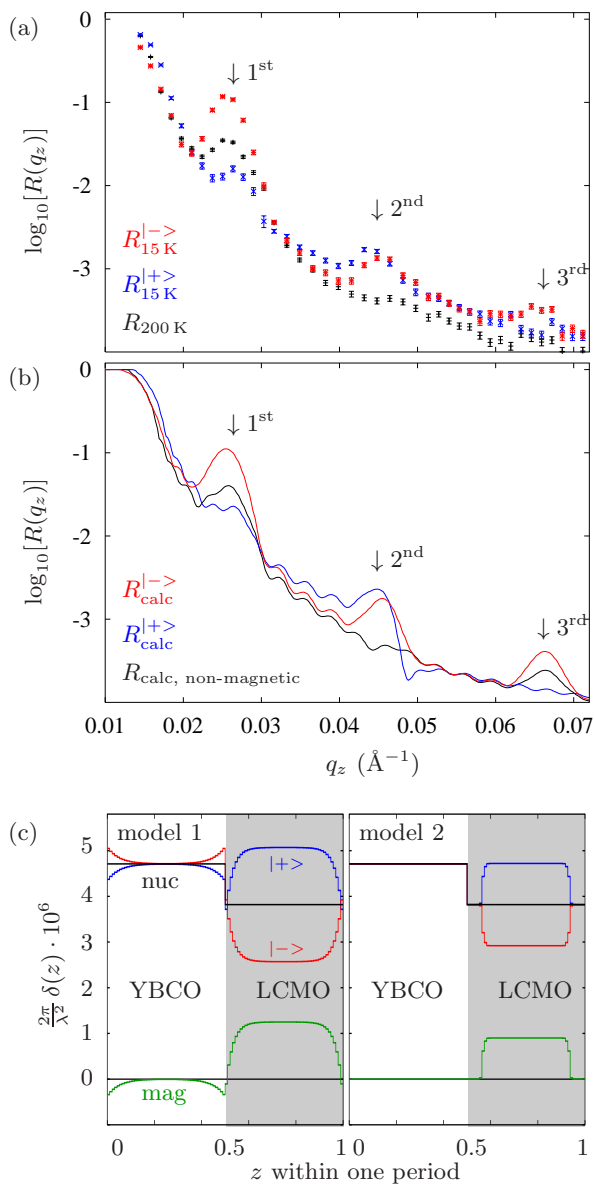


FIG. 2: (a) Polarized specular reflectivity of sample 2 at 200 and 15 K, for  $H_{\text{ext}} = 100$  Oe (field cooled). (b) Simulated reflectivity curves (model 1) and (c) model potentials that reproduce the experimental data. *Left*: inverse proximity effect (model 1) and *right*: “dead layer” (model 2).  $\delta(z) \propto V(z)$  is the deviation of the refractive index from 1,  $\lambda$  is the neutron wavelength.

netization data) and the magnetic penetration depth of the superconductor is very large for this field orientation, the electromagnetic coupling between FM and SC is also expected to be negligible.

In contrast, model 1 describes a situation where the SC and FM order parameters are in close contact and thus are likely to experience a strong mutual interaction. Interestingly, the essential feature of model 1, that is, a thin layer on the SC side which has a net magnetic moment oriented antiparallel to the one in the FM layer,

has recently been proposed theoretically [12]. According to this theory, the unusual magnetization profile near the interface originates from Cooper pairs that have a finite overlap with both the FM and the SC layers. Heuristically, the preferential spin alignment of one electron in the FM layer leads to an antiparallel spin orientation of the second electron of the spin-singlet pair that resides in the SC layer. While phase-coherent Cooper pairs exist only in the SC state, *i.e.* for  $T < T_{\text{sc}}$ , similar arguments apply for other kinds of itinerant spin-singlet pairs. The existence of spin-singlet pairs at elevated temperatures  $T > T_{\text{sc}}$  has been indeed proposed in the context of the unusual normal state electronic properties of the cuprate HTSC (so-called pseudogap phenomenon) [13]. Our data are also consistent with recent macroscopic magnetization measurements suggesting an antiferromagnetic component of the magnetization profile at the YBCO/LCMO interface [14]. Underdoped cuprates are known to be susceptible to antiferromagnetic order, and a staggered magnetization profile whose amplitude decreases as a function of distance from the interface would generate a net magnetization in YBCO, as observed.

In summary, our neutron reflectometry measurements on high-quality  $\text{YBa}_2\text{Cu}_3\text{O}_7/\text{La}_{2/3}\text{Ca}_{1/3}\text{MnO}_3$  multilayers have revealed detailed, microscopic information about the magnetization profile as a function of in-plane and out-of-plane wave vectors. The pronounced modification of this profile at the superconducting transition indicates a significant proximity coupling between SC and FM order parameters, likely due to exchange interactions. The findings are discussed in terms of the recently predicted inverse proximity effect [12].

We acknowledge M. Wolff for support on ADAM at ILL, France. This work was partly performed at Morphéus at SINQ, Paul Scherrer Institute, Switzerland.

- 
- [1] C.L. Chen and D. H. Reich, *JMMM* **200**, 83 (1999); A.M. Goldman *et al.*, *ibid.* **200**, 69 (1999).
  - [2] Y.A. Izyumov, Y.N. Proshin, M.G. Khusainov, *Physics-Uspekhi* **45**, 109 (2002); L.N. Bulaevskii, *et al.*, *Adv. Phys.* **34**, 175 (1985).
  - [3] V.V. Ryazanov *et al.*, *Phys. Rev. Lett.* **86**, 2427 (2001); T. Kontos *et al.*, *ibid.* **86**, 304 (2001).
  - [4] Z. Sefrioui *et al.*, *Appl. Phys. Lett.* **81**, 4568 (2002); Z. Sefrioui *et al.*, *Phys. Rev. B* **67**, 214511 (2003).
  - [5] H.U. Habermaier *et al.*, *Physica C* **364**, 298 (2001); T. Holden *et al.*, *Phys. Rev. B* **69**, 064505 (2004).
  - [6] G.P. Felcher, *J. Appl. Phys.* **87**, 5431 (2000); H. Zabel and K. Theis-Bröhl, *J. Phys.: Condens. Matter* **15**, S505 (2003).
  - [7] V. Holý, U. Pietsch, T. Baumbach, *High-Resolution X-Ray Scattering from Thin Films and Multilayers* (Springer Tracts in Modern Physics, Vol. 149); P. Mikulík, EDXR — X-ray and neutron reflectivity calculation program, 2001, mikulik@physics.muni.cz.

- [8] C.A.R. Sá de Melo, Phys. Rev. Lett. **79**, 1933 (1997).
- [9] Z. Radovic *et al.*, Clem, Phys. Rev. B **38**, 2388 (1988); Z. Radovic *et al.*, *ibid.* **44**, 759 (1991).
- [10] A.I. Buzdin, and L.N. Bulaevskii, Sov. Phys. JETP **67**, 576 (1988); F.S. Bergeret, K.B. Efetov, and A.I. Larkin, Phys. Rev. B **62**, 11872 (2000).
- [11] A.I. Buzdin, and A.S. Melnikov, Phys. Rev. B **67**, 020503 (2003); A.F. Volkov *et al.*, Phys. Rev. Lett. **90**, 117006 (2003).
- [12] F.S. Bergeret, A.F. Volkov, and K.B. Efetov, Phys. Rev. B **69**, 174504 (2004).
- [13] P.W. Anderson, Science **235**, 1196 (1987); P.W. Anderson, *The Theory of Superconductivity in the High-Tc Cuprates*, Princeton Univ. Press (1997).
- [14] N. Haberkorn *et al.*, Appl. Phys. Lett. **84**, 3927 (2004); P. Przyslupski *et al.*, Phys. Rev. B **69**, 134428 (2004).